

BEHAVIOR OF RECTANGULAR CONCRETE FILLED STEEL TUBES SUBJECTED TO TORSION

M.A. KOTAB¹, H. M. RAMADAN² AND S.A. MOURAD³

ABSTRACT

An analytical study using finite element modeling is conducted to investigate the structural behavior of rectangular concrete-filled steel tubes (RCFST) under torsion. A comprehensive parametric study is carried out to evaluate the effect of various variables on torsional capacity of RCFST sections. The following parameters are considered; steel strength, steel ratio, and dimensions of steel section. The results are also compared to the design equation presented by the available international codes.

KEYWORDS: Rectangular concrete filled tubes, torsion, finite element modeling.

1. INTRODUCTION

Concrete-Filled steel tubes, CFST, have been widely used and became increasingly popular in structural applications since they have several advantages in the field of construction and design. They have excellent earthquake resistant properties due to their high strength, ductility and large energy absorption capacity resulting from composite action between the constituent elements. Additionally, the confinement created by steel casing enhances the concrete properties by putting it under a tri axial state of stress. Also the section stability strength is increased by preventing the inward buckling of the steel tube. Among other advantages of CFST columns are; speed of construction, saving formwork for the concrete core, and possible use of simple standardized connections [1, 2]. In addition to the interaction

¹ Graduate Student, Structural Engineering Department, mahspeed@hotmail.com

² Associate Professor, Structural Engineering Department, Faculty of Engineering, Cairo University, Drhazem2003@yahoo.com

³ Professor, Structural Engineering Department, Faculty of Engineering, Cairo University, Smourad@eng.cu.edu.eg

between steel and concrete, the steel tube and the concrete in the cross section are positioned so that the efficiency of the section can be optimized. The steel tube that has a much greater modulus of elasticity than the concrete is located at the outer perimeter so it most effectively contributes to the moment of inertia of the section. Both good strength and ductility make this system as the viable alternative for application in tall buildings located in high seismic zones [3, 4].

Previous studies have focused on a better understanding of the behavior of concrete-filled tubes under axial load and bending [5-7]. Little research has paid attention to study the behavior of the concrete-filled tubes under torsion [8-10]. There are no provisions for concrete-filled tubes under torsion in the specification issued by AISC [11]. However, the torsion effect may not be neglected in some cases particularly for eccentrically loaded members. Therefore, it is important to understand the behavior of concrete-filled tubes under torsion. In this study, a numerical investigation was carried out to study the behavior and design of thin-walled concrete-filled steel tubes under torsion.

In order to investigate the ultimate torsion strength of RCFST sections using the finite element technique, several models with different rectangular box sections were constructed and analyzed using ANSYS software [12]. A parametric study has been conducted considering the following parameters: Section aspect ratio defined by the section width to its depth, steel ratio defined by the ratio of steel area to the concrete area and steel yield stress. All specimens are assumed to have the same length.

2. FINITE ELEMENT MODELING

2.1 Steel Tube

Four-node shell elements (SHELL 181) are used to simulate the rectangular steel tube. The element is well-suited for linear, large rotation, and/or large strain nonlinear applications and is recommended for many problems that have convergence difficulty. Figure 1 shows the finite element mesh of a concrete-filled steel square tube. Different mesh sizes were tried in order to find a reasonable mesh that provides both accurate results and reasonable computational time. In the finite element model,

elastic–plastic model was used to describe the constitutive behavior of the steel. The steel Young’s modulus is taken as 210,000 MPa and Poisson’s ratio is assumed to be 0.30. To avoid any distortion at load application side, a thick plate is assumed to be attached connecting all nodes at load application face as shown in Fig.1

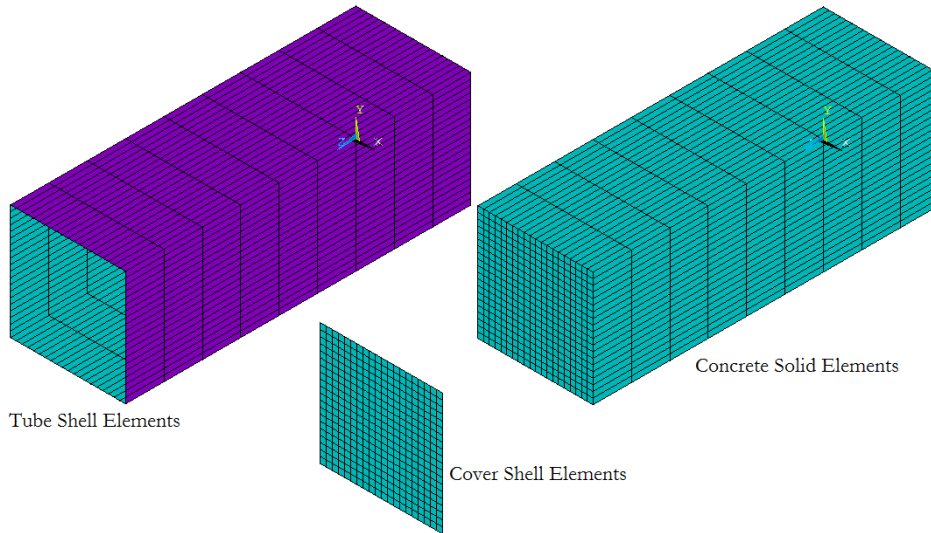


Fig. 1. Finite element meshing of the concrete-filled steel tube.

2.2 Filling Concrete

Three dimensional structural solid element (SOLID65) is used to simulate the concrete in-fill as shown in Fig.1. The solid element is capable of cracking in tension and crushing in compression. The most important aspect of this element is the treatment with nonlinear material properties since the concrete is capable of cracking (in three orthogonal directions), crushing, plastic deformation, and creep. Modeling of reinforced concrete using finite element methods is not straight forward since concrete does not have well-defined constitutive properties. Both linear and nonlinear material models were used for SOLID65 elements. The concrete tensile strength was estimated as 0.1 of the concrete compressive strength. Poisson’s ratio of concrete is taken as 0.2. Shear transfer coefficients for open and closed cracks were set to 0.2 and 0.6, respectively. The value of the stiffness multiplier for cracked tensile condition was taken as the default value 0.6. Based on Section 8.5.1 in ACI 318m-05 [13], the concrete modulus of elasticity is calculated using the following equation:

$$E_c = 4700 \sqrt{f_c'} \quad (1)$$

Where: f_c' is the uniaxial compressive stress. The ANSYS program [12] requires the uniaxial stress-strain relationship for concrete in compression. ANSYS crushing option does not work properly for models containing plain concrete. Hence, the “crushing” option is removed to overcome the convergence problems and the concrete plasticity in the compression zone is modeled using von Mises plasticity multi-linear option. This might cause some minor inaccuracy of the results; however, it was done in order to save computational time while focusing upon the results of the steel components. The well-known uniaxial stress-strain curve shown in Fig. 2, proposed earlier [14], is used in this study:

$$\sigma(\varepsilon) = \frac{E_c \varepsilon}{1 + \left(\frac{\varepsilon}{\varepsilon_o}\right)^2} \quad (2)$$

$$\varepsilon_o = \frac{2f_c'}{E_c} \quad (3)$$

Where: $\sigma(\varepsilon)$ is stress value at any given strain (ε) and ε_o is strain at the ultimate compressive stress f_c' .

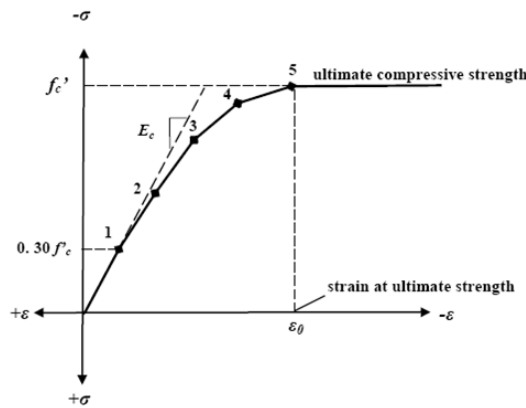


Fig. 2. Simplified compressive uniaxial stress-strain curve for concrete [14].

2.3 Concrete – Steel Tube Interface

The interface between steel tube and concrete infill is modeled using contact pairs: the target element, TARGE170, and the contact element, CONTA173. The

TARGE170 element is used to overlay the solid elements of the concrete core. Meanwhile, the CONTA173 element is used to overlay the inside areas of the shell elements modeling the steel tube. These two elements are able to model surface-to-surface contact between shell elements for the steel tube and solid elements for the concrete fill. The stiffness between the surface and target can be modified to define the bond characteristics. The coefficient of friction, μ , was chosen equal to 0.25 [8]. In this analysis, the initial bond behavior of the contact pairs is assumed to be fully bonded by setting KEYOPT (12) of CONTA173 elements to 5. The stiffness is updated after each iteration by changing KEYOPT (10) to a value of 2. While constructing the model, an initial gap is set between the concrete and tube. This gap is insignificant, but potentially is not detrimental to the analysis. KEYOPT (9) and (5) is set to 1 in order to neglect the initial gap. Meanwhile, default values of the real constants are used for the contact pair except for the value of normal penalty stiffness factor (FKN) and the penetration tolerance factor (FTOLN). They are set to 0.1 and 0.01, respectively.

2.4 Loads and Boundary Condition

The load is applied as concentrated torsional moment at one of the column ends and the other end is restrained against movements as shown in Fig. 3. ANSYS employs the “Newton-Raphson” approach to solve nonlinear problems. Consequently, the applied load is divided into a series of load increments which are applied over load steps. The maximum numbers of iteration is maximized to 200 in a sub-step. In addition, the force label convergence criteria are softened (normalized value is set from 1% to 5%). Displacement control strategy is adopted due to the softening behavior of concrete. Test analyses were first performed in order to establish the sensitivity of the results to mesh size. Finer mesh sizes yields more accurate results. However, at a certain level, there will be no significant variation in results.

2.5 Verification of Finite Element Model

The torsional capacities predicted using the FEA modeling described as above are compared with previously published test results [15]. The dimensions of tested

square steel tube are 400mm width, 1200mm length and 9.30mm thickness. The steel yield stress is 345MPa however the concrete ultimate strength is 50MPa. The predicted torsional moment, T , versus rotation angle, Θ , are compared and presented through Fig. 4. It is observed that there are differences of about 3% between the numerical and experimental responses which indicate good agreement is obtained between the predicted and tested results. This difference may be attributed to the uncertainty in the material properties and the approximations considered in modeling.

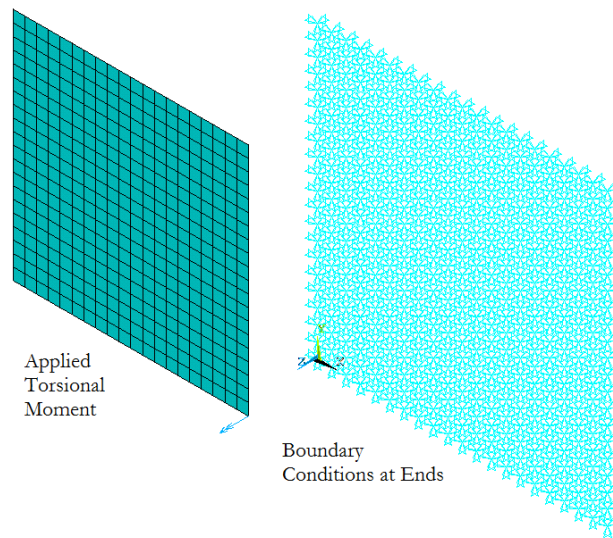


Fig. 3. Applied Boundary Conditions.

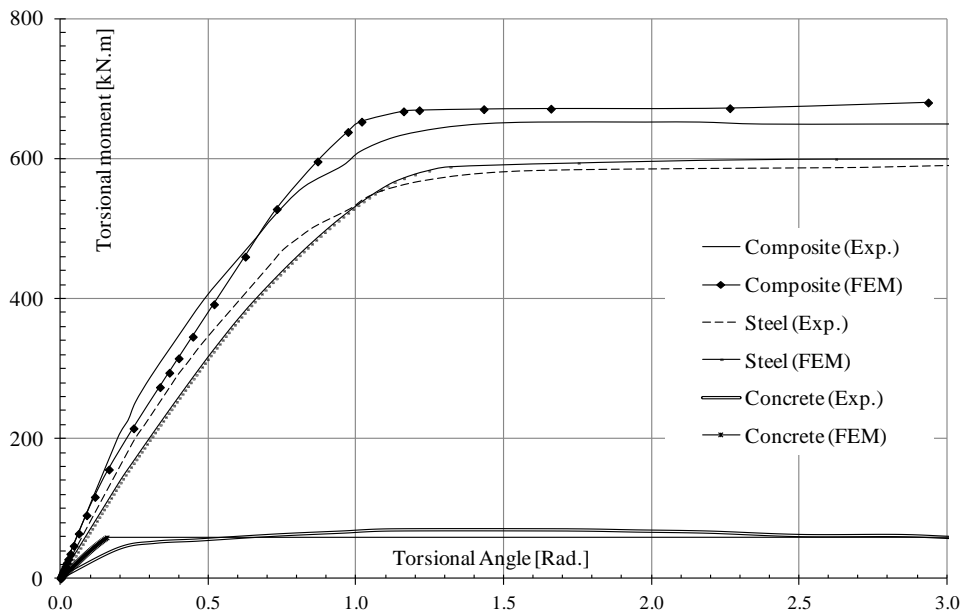


Fig. 4. Experimental and Numerical Results for Specimen CFT 7 [15].

3. PARAMETRIC STUDY

The objective of this research is to study the structural behavior of rectangular concrete-filled steel tube (RCFST) with application of uniform torsion loading to the free surface. Parametric study is conducted to investigate the effect of various variables on torsional capacity of RCFST sections. The variables considered are shown in Table 1 and summarized as follows: rectangular steel section aspect ratio, steel ratio, steel strength, and concrete strength. Rectangular steel section aspect ratio, B/D , defined by the section width, B , to the section depth, D , is taken to be from 1 to 2. Steel ratio, α , defined by the ratio of steel area to the concrete area is assumed to be changed from 0.05 to 0.2. Three values of steel yield stress, F_y , are considered for the steel sections 235, 345 and 420MPa. Concrete compressive strength is assumed to be 60Mpa. All elements, loading and boundary conditions used through the finite element analysis are similar to those used in verification model to ensure the output results of this parametric study. Length and thickness of steel tubes are fixed for all models to be 1200mm and 10mm, respectively. The chosen thickness gives a maximum B/T ratio of 88 which is less than to avoid local buckling effect.

Table 1. Range of Paramters Studied.

RCFST Dimensions (BxD) mm	B/D	Steel ratio (α)	Fy [MPa]
400x400, 600x400 & 800x400	1, 1.5 & 2	0.05, 0.1, 0.15 & 0.2	235, 345 & 420

3.1 Moment –Rotation Curves of CFST Sections

Figures 5 through 13 show the applied torsional moment-rotation relationship for RCFST sections having different steel yield strengths and steel ratios. The following comments can be written:

- All moment-rotation curves are characterized by three stages:
 - Elastic stage at which torsional behavior of the RCFST section increases linearly with high values of stiffness in the early stage of loading. Elastic torsional moment in the linear stage increases with increase of column aspect ratio.

- Elastic-plastic stage which represents the curved part after the linear stage. During this stage with the increase of torsional moment, the concrete core will begin to crack and increase in volume leading to increase of confinement provided by the outer steel tube.
- Strain hardening stage which shows large slips at incrementally constant Torque after reaching of the peak torque load. During this stage, RCFST sections have not any potential in resisting the torsional moment due to the strain hardening effect of steel and concrete cracking.
- The torsional moment capacity of rectangular RCFST sections increases proportionally with increasing steel ratio, steel yield strength and aspect ratios. The capacity increase 50% on average when steel ratio increases from 0.1 to 0.15. Such increase reaches 80% and 250% when aspect ratio increases from 1.0 to 1.5 and 2.0, respectively. Also the torsional strength of member increases by 40% when f_y increases from 235 MPa to 345 MPa and by 19% when f_y increase from 345 MPa to 420 MPa. This is due to the fact that steel section composed of high grade steel can support higher torsional moment having the same confined concrete compressive strength inside.

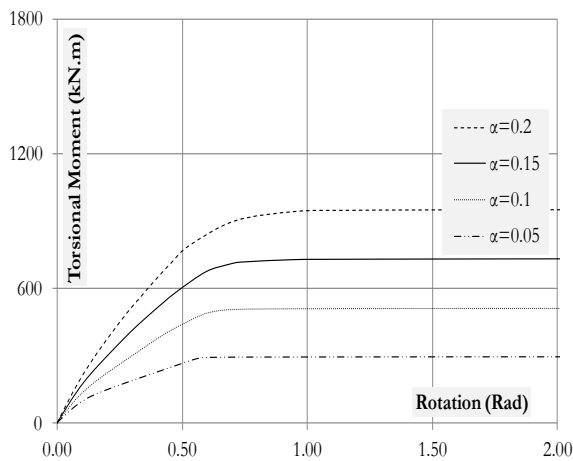


Fig. 5. Torsional Monent-Rotation, B/D=1.0, $F_y=235\text{MPa}$.

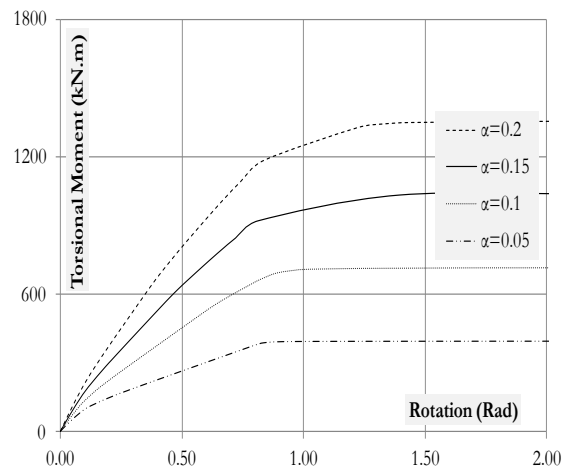


Fig. 6. Torsional Monent-Rotation, B/D=1.0, $F_y=345\text{MPa}$.

BEHAVIOR OF RECTANGULAR CONCRETE FILLED ...

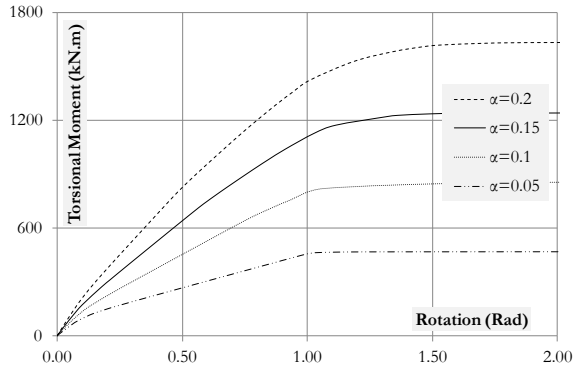


Fig. 7. Torsional Moment-Rotation, $B/D=1.0$, $F_y=420\text{MPa}$.

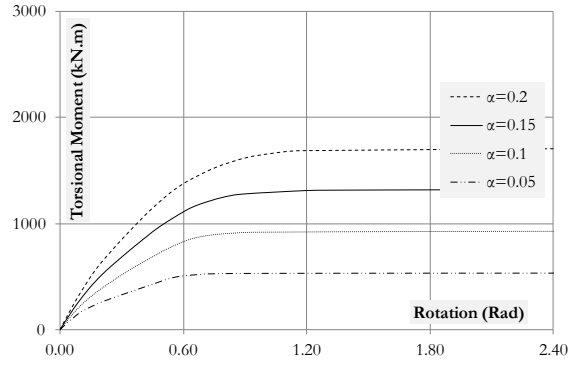


Fig. 8. Torsional Moment-Rotation, $B/D=1.5$, $F_y=235\text{MPa}$.

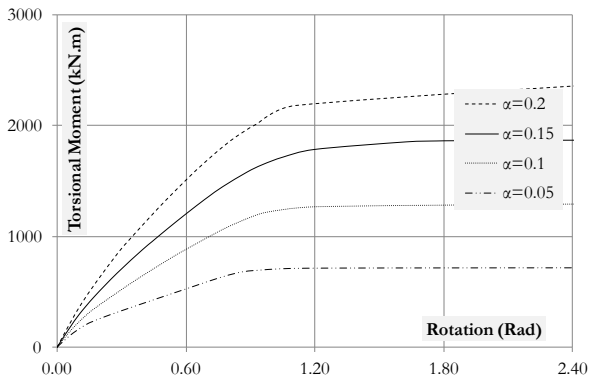


Fig. 9. Torsional Moment-Rotation, $B/D=1.5$, $F_y=345\text{MPa}$.

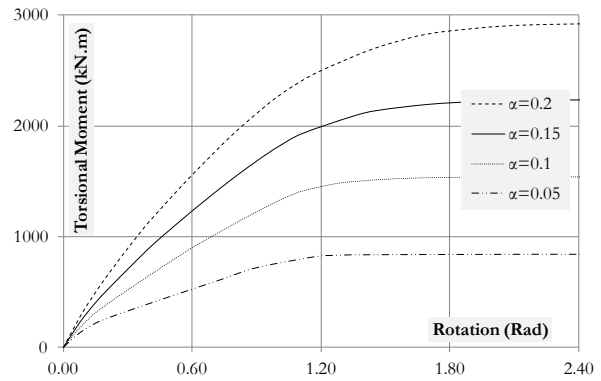


Fig. 10. Torsional Moment-Rotation, $B/D=1.5$, $F_y=420\text{MPa}$.

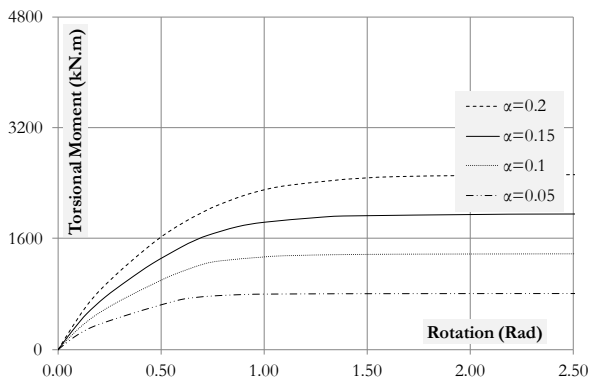


Fig. 11. Torsional Moment-Rotation, $B/D=2.0$, $F_y=235\text{MPa}$.

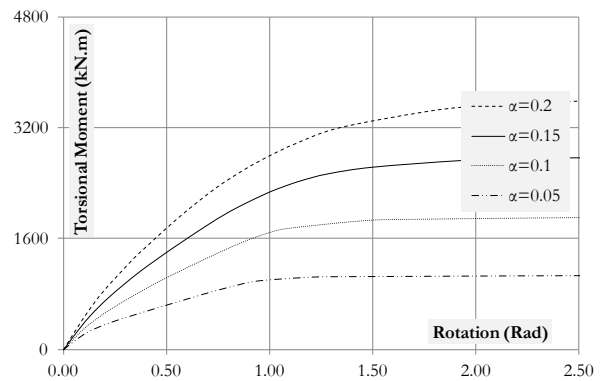


Fig. 12. Torsional Moment-Rotation, $B/D=2.0$, $F_y=345\text{MPa}$.

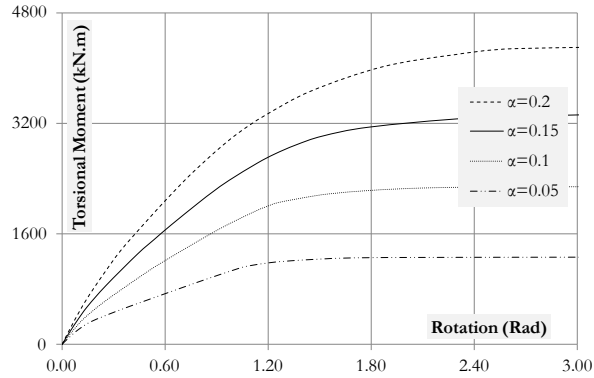


Fig. 13. Torsional Moment-Rotation, B/D=2.0, $F_y=420\text{MPa}$.

3.2 Initial Stiffness of RCFST Sections Torsional Behavior

Figure 14 shows variation of the initial stiffness values at linear stage and determined from the analysis versus RCFST aspect ratios for different values of sections yield stress and assuming steel ratio equal to 0.1. Figure 15 shows the effect of steel ratios on the initial stiffness. It is clear that all curves coincide by changing steel yield strength which indicates that initial stiffness is not affected by steel material grade. Also it is found that initial stiffness is proportional linearly to the aspect ratios with maximum values corresponding to application of highest steel ratio. Increasing the section aspect ratio results in a great increase of the initial stiffness reaching to 150% corresponding to ratio increase from 1.0 to 2.0.

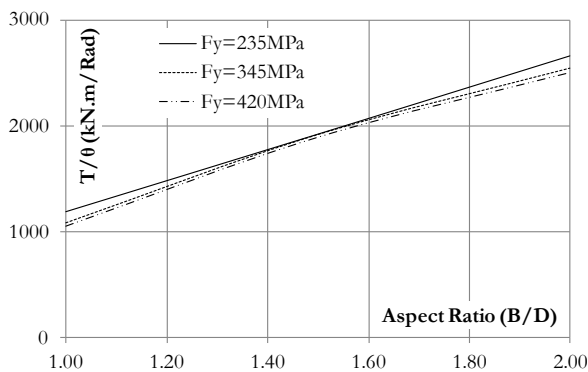


Fig. 14. Effect of steel yield strength on initial stiffness.

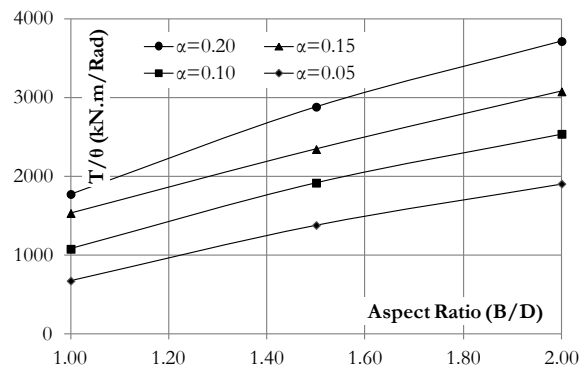


Fig. 15. Effect of steel ratios on initial stiffness.

3.3 Final Stiffness of RCFST Sections Torsional Behavior

Figures 16 and 17 show the variation of final torsional-rotational stiffness of RCFST sections with column aspect ratio considering different values of steel yield strength and aspect ratios. It is shown that final torsional-rotational stiffness increases with increase of section aspect ratios, steel ratios and steel yield strength. The increase reaches 40 % for aspect ratio from 1.0 to 2.0. Also the percentage of increase is 15% on average when steel yield strength changes from 235 MPa to 345 MPa. Increasing the steel yield strength to 420 MPa leads to further increase of the stiffness estimated by 35%. Torsional Stiffness increase by increasing steel yield strength is due to the fact that steel with high grade provide more resistance to torsion. This percentage increase reaches 80% and 120% for steel ratio changing from 0.05 to 0.1 and 0.15 to 0.2, respectively.

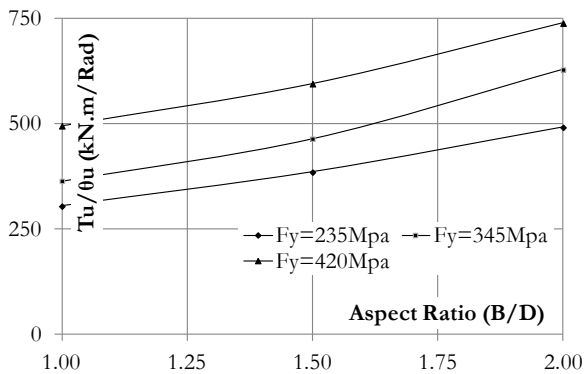


Fig. 16. Effect of steel yield strength on final torsional stiffness at $\alpha=0.10$.

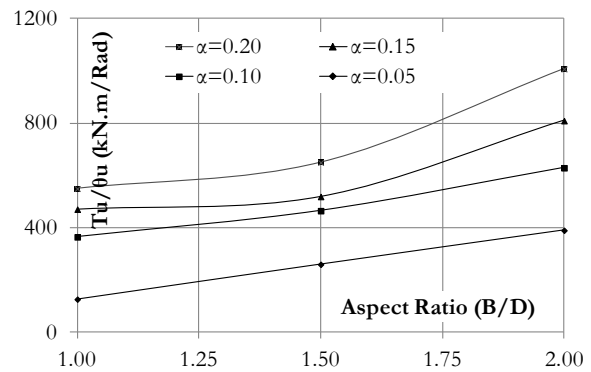


Fig. 17. Effect of steel ratios on final torsional stiffness at $F_y=345$ MPa.

3.4 Effect of Steel Yield Strength on CFST Sections Torsional Behavior

Figure 18 illustrates the variation of T_u/T_p with α for column aspect ratio set to 1.0 on different steel yield strength. The torsional strength obtained from the finite element analysis, T_u , was normalized to the theoretical plastic torsional strength of hollow steel box section, T_p , calculated according to AISC standard [11] in order to present the results in non-dimensional form. Assuming that shear forces are uniformly distributed over the thickness and neglecting warping, AISC formula is presented by:

$$T_p = 2A_o \tau_y t \quad (4)$$

Where A_o : area enclosed by shape, measured to centerline of thickness of bounding element, t is thickness of bounding element, and τ_y is shear yielding stress of steel taken as $F_y/\sqrt{3}$. Figures 19 and 20 show the same variation but for another values of aspect ratios taken 1.5 and 2.0, respectively. The following comments can be written:

- The values of T_u/T_p ratios are always greater than unity since T_u is larger than T_p due to the existing of core concrete leading to enhancement of structural behavior of RCFST sections that subjected to torsion.
- A Comparison of results revealed that RCFST sections with different aspect ratios having the same steel ratio and yield strength the values of T_u/T_p change slightly. Also it can be seen that the higher values of the steel ratio, α , and the steel yielding strength F_y , the lower values of T_u/T_p ratios. This is attributed to the fact that the values of T_p increase faster than T_u with the increase of α or F_y and thus leads to a reduction of the ratio of T_u/T_p . This leads to a higher contribution of the steel in RCFST under torsion loading. At aspect ratio equals to 1.0 and increase of F_y from 235 to 420 MPa, the value of T_u/T_p ratio was reduced from 1.18 to 1.1 and 1.096 to 1.054 at α equals to 0.1 and 0.2, respectively. This indicates that the rate of reduction in value T_u/T_p was decreased from 8% to 4% with the increase of α from 0.1 to 0.2.

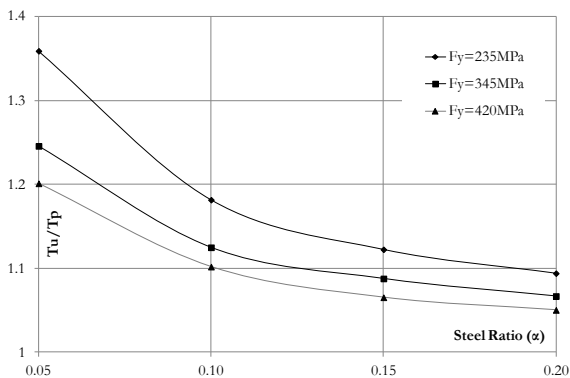


Fig. 18. T_u/T_p versus α [B/D=1.0].

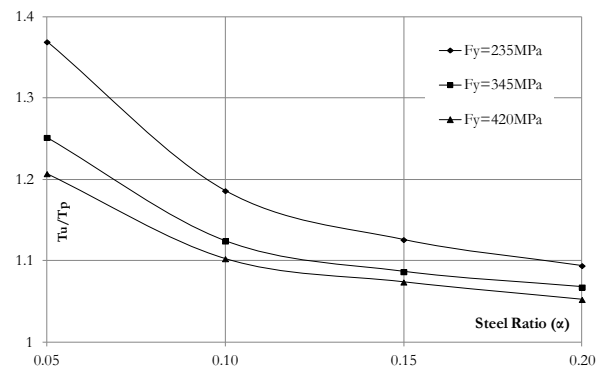


Fig. 19. T_u/T_p versus α [B/D=1.5].

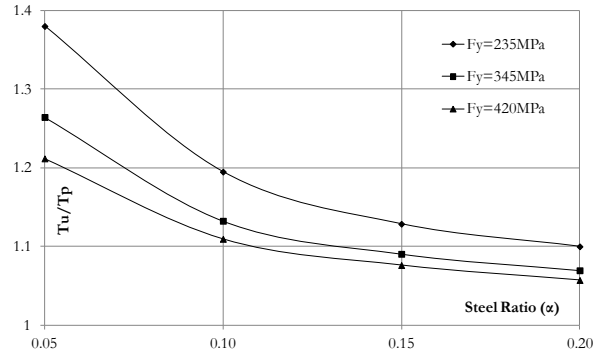


Fig. 20. T_u/T_p versus α [$B/D=2.0$].

3.5 Development of Simple Formulas

Regression analysis is considered the most common statistical modeling technique, and it is suitable for the majority of problems. Therefore, regression analysis has been performed using finite element modeling results to analyze and investigate the ultimate torsion strength of RCFST sections. It is aimed to develop practical equations and charts estimating the ultimate torsion strength, T_u , of composite section in terms of non-dimensional form T_u/T_p whereas the, T_p , represents the plastic torsional strength of corresponding hollow steel sections when subjected to pure torsion. Results presented in previous figures and conclusions drawn from the study carried out through the previous discussion indicate that the torsional capacity of RCFST sections depends mainly on steel ratios and yield strength of steel section. These parameters were taken as variables to obtain simplified formulas of polynomial to the third order established for different steel ratios. All regression analysis trials are made using excel to obtain simplified equation as shown in Fig. 21 through 23. It is shown that the design equation predicts RCFST sections torsional strength accurately with approximately 1% errors which is practically accepted.

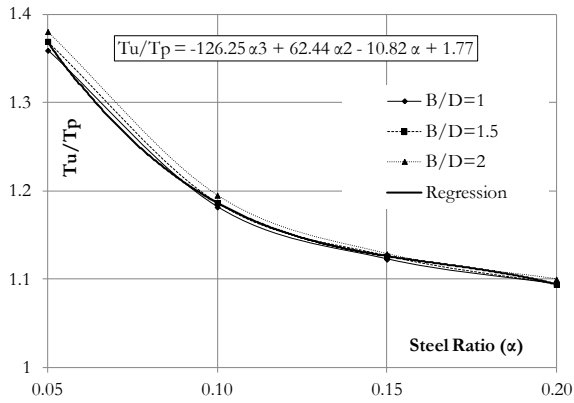


Fig. 21. T_u/T_p versus α [$F_y=235\text{Mpa}$].

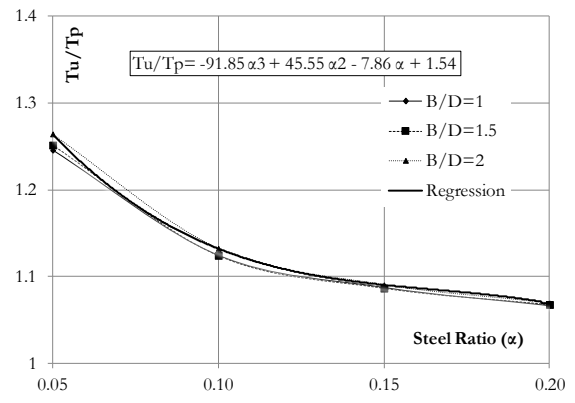


Fig. 22. T_u/T_p versus α [$F_y=345\text{Mpa}$].

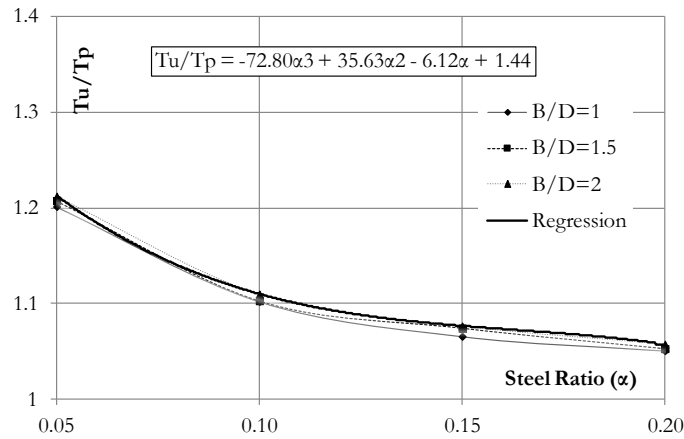


Fig. 23. T_u/T_p versus α [$F_y=420\text{Mpa}$].

4. CONCLUSION

The present study is an attempt to study the torsional behavior of RCFST. The following observations and conclusions can be highlighted.

- Results revealed that RCFST sections with different aspect ratios having the same steel ratio and yield strength the values of T_u/T_p change slightly.
- The higher the values of the steel ratio, α , and the steel yielding strength F_y , the lower the values of T_u/T_p ratios. This is expected since the values of T_p increase faster than T_u with the increase of α or F_y due to higher contribution of the steel in RCFST under torsion loading and thus leads to a reduction of the ratio of T_u/T_p .
- The torsional moment capacity of RCFST sections increases proportionally with increasing steel ratio, steel yield strength and aspect ratios.

- The initial torsional stiffness is not affected by changing the steel yield strength and increases linearly with the increase of the section aspect ratios.
- The final torsional-rotational stiffness increases with increase of section aspect ratios, steel ratios and steel yield strength. The increase reaches to 40 % for increase of section aspect ratio from 1.0 to 2.0. Also the percentage of increase is 15% on average for steel yield strength changing from 235 MPa to 345 MPa. Increasing the steel yield strength to 420 MPa leads to further increase of the stiffness estimated by 35%. Torsional Stiffness increase by increasing steel yield strength is due to the fact that steel with high grade provide more resistance to torsion. This percentage increase ratio reaches to 80% and 120% for steel ratio changes from 0.05 to 0.1 and 0.15 to 0.2, respectively.

REFERENCES

1. Shams, M., and Saadeghvaziri, M.A., "State of the Art of Concrete-Filled Steel Tubular Columns". ACI J; Vol. 94, No. 5, pp. 558-71, 1997.
2. Kilpatrick, A. E., and Rangan, B.V., "Influence of Interfacial Shear Transfer on Behavior of Concrete Filled Steel Tubular Columns". ACI Journal, Vol. 96, No. 4, pp. 642-648, 1999.
3. Young-Hwan, C., "A modified AISC P-M Interaction Curve for Square Concrete Filled Tube Beam-Column", University of Illinois at Urbana-Champaign, USA, 2004.
4. Uchikoshi, M., Hayashi, Y., and Morino, S., 2000,"Mertis of CFT Column System Results of Trial Design of Theme Structures", Proc. of 6th ASCCS, Composite and Hybrid Structural Institute of Japan, No. 4, In Japanese, 2000.
5. Munoz, P. R. and Thomas, C- T., "Biaxial Loaded Concrete- Encased Composite column Design Equation", ASCE, Journal of Struct. Eng., Vol. 123, No. 12, pp. 1576-1585, 1997.
6. Schneider, S.P., "Axially loaded Concrete-Filled Steel Tubes", ASCE, Journal of Structure Engineering, Vol. 124, No. 10, 1998.
7. Martin, D., and Russell, Q., "Design of Circular Thin- Walled Concrete Filled Steel Tubes", ASCE, J. Struct Eng., Vol. 126, No. 11, pp. 1295-1303.
8. Han, L.-H., Yao, G.-H., and Tao, Z., "Performance of Concrete-Filled Thin-Walled Steel Tubes under Pure Torsion." Thin-Walled Structures, Vol. 45, pp. 24-36, 2007.
9. Han, L.-H., Yao, G.-H., and Tao, Z., "Behavior of Concrete-Filled Steel Tubular Members Subjected to Combined Loading." Thin-Walled Struct., Vol. 45, pp. 600-619, 2007.

10. Juan, J., Jin, W.L., "Design of Thin- Walled Centrifugal Concrete- Filled Steel Tubes under Torsion", Thin- Walled Structures, China, Vol. 47, pp. 271-276, 2009.
11. AISC 360-05. American Institute for Steel Construction.
12. ANSYS. "ANSYS Release 12.0 Documentation. SAS IP Inc., 2007."
13. ACI 318-05. "Building Code Requirements for Structural Concrete ACI Committee 318 and Commentary (318R-05)", Farmington Hills: American Concrete Institute, 2005.
14. Desayi, P., and Krishnan., S., Equation for the Stress Strain Curve of Concrete, ACI Journal, Proc., Vol. 61, No. 3, pp. 345-350, 1964.
15. Beck, J., and Kiyomiya, O., 2003, "Fundamental Pure Torsional Properties of Concrete Filled Circular Steel Tubes". J. Mater Conc. Struct. Pavements, JSCE No. 739/V-60, pp. 85-96, 2003.

سلوك الانابيب الصلب المملوءة بالخرسانة المعرضة لعزوم اللي

يتناول البحث سلوك المواسير الصلب المملوءة بالخرسانة المعرضة لعزوم اللي بعمل نماذج تحليلية لشكل قطاع مستطيلي مركب بواسطة برامج العناصر المحددة اخذا في الاعتبار السلوك اللاخطي لتلك القطاعات وتم تحليل النتائج ومقارنتها مع التجارب المعملية من اجل الوصول الى توصيات مفيدة للمهندس المصمم بالإضافة الى عمل دراسة بارامترية لتحديد تأثير الخواص الهندسية المختلفة للقطاع المركب على المقاومة القصوى لعزوم اللي وتم التوصل إلى منحنيات تصميمية ومعادلات لأشكال القطاعات المستطيلة المختلفة.